thermochemical energy scale.[15] The more reactive oxoiron porphyrin systems[16] are under current investigation.

Received: June 8, 2000 [Z15242]

[1] a) B. Meunier in *Biomimetic Oxidations Catalyzed by Transition Metal Complexes* (Ed.: B. Meunier), Imperial College Press, London, **2000**, pp. 171–214; b) J. L. McLain, J. Lee, J. T. Groves in *Biomimetic Oxidations Catalyzed by Transition Metal Complexes* (Ed.: B. Meunier), Imperial College Press, London, **2000**, pp. 91–170.

[2] a) B. Meunier, *Chem. Rev.* **1992**, 92, 1411–1456; b) J. T. Groves, K. Shalyaev, J. Lee in *The Porphyrin Handbook*, *Vol. 4* (Eds.: K. M. Kadish, K. M. Smith, R. Guilard), Academic Press, San Diego, **2000**, pp. 17–40.

[3] a) J. T. Groves, J. Lee, S. S. Marla, *J. Am. Chem. Soc.* **1997**, *119*, 6269–6273; b) N. Jin, J. T. Groves, *J. Am. Chem. Soc.* **1999**, *121*, 2923–2924; c) C. G. Miller, S. W. Gordon-Wylie, C. P. Horwitz, S. A. Strazisar, D. K. Peraino, G. R. Clark, S. T. Weintraub, T. J. Collins, *J. Am. Chem. Soc*, **1998**, *120*, 11540–11541; d) F. M. MacDonnell, N. L. P. Fackler, C. Stern, T. V. O'Halloran, *J. Am. Chem. Soc.* **1994**, *116*, 7431–7432.

[4] a) B. W. Griffin in *Peroxidases in Chemistry and Biology*, *Vol. 2* (Eds.: J. Everse, K. E. Everse, M. B. Grisham), CRC Press, Boca Raton, FL, **1991**, pp. 85–138; b) A. Butler, J. V. Walker, *Chem. Rev.* **1993**, *93*, 1937–1944; c) G. Labat, B. Meunier, *J. Chem. Soc. Chem. Commun.* **1990**, 1414–1416; d) H.-A. Wagenknecht, C. Claude, W. D. Woggon, *Helv. Chim. Acta.* **1998**, *81*, 1506–1520.

[5] Mn^{III}TM-2-PyP was purchased from Mid-century, Posen, IL, and was further purified. Its concentration was standardized spectrophotometrically using $\varepsilon = 129000\ cm^{-1}M^{-1}$; I. Batinic-Haberle, L. Benov, I. F. Spasojevic, I. Fridovich, *J. Biol. Chem.* **1998**, *273*, 24521–24528.

[6] T. Mussini, G. Faita in *Encyclopedia of Electro- chemistry of the Elements*, *Vol. 1* (Ed.: A. J. Bard), Marcel Dekker, New York, **1973**, p. 11 and p. 64.

[7] Solutions of $HOBr^-/OBr^-$ that were free of Br^- were prepared by mixing equimolar amounts of OCl^- and Br^-; M. Gazda, D. W. Margerum, *Inorg. Chem*. **1994**, *33*, 118–123.

[8] A buffered (pH 7.0, 25 mM phosphate buffer) solution of 10 μM (**2**), 5 mM NaBr, and 50 μM phenol red had 100 μM HSO_5^- added, resulting in production of bromophenol blue (yield 30%, $\lambda_{abs} = 592$ nm) within 1 s. In the absence of catalyst, control experiments showed less than 1% production of bromophenol blue within 1 min.

[9] P. G. Furtmüller, U. Burner, C. Obinger, *Biochemistry* **1998**, *37*, 17923–17930.

[10] A. Butler, A. H. Baldwin, *Struct. Bonding (Berlin)* **1997**, *89*, 109–132, and references therein.

[11] The dioxo nature of **1** at pH 12–14 was first suggested by Su et al. F. C. Chen, S. H. Cheng, C. H. Yu, M. H. Liu, Y. O. Su, *J. Electroanal. Chem.* **1999**, *474*, 52–59.

[12] The second protonation can occur either on the hydroxo ligand affording an oxo–aqua species (shown in Scheme 1) or on the oxo ligand giving a dihydroxo species. Our results support the oxo–hydroxo tautomerism mechanism proposed by Meunier to explain the solvent oxygen incorporation to substrate in manganese porphyrin catalyzed processes. J. Bernadou, B. Meunier, *Chem. Commun.* **1998**, *20*, 2167–2173.

[13] In the pH region investigated, the reverse reaction rate constant, k_r was found to be first order in both $c_{Mn^{III}}$ and c_{OBr^-+HOBr}.

[14] In a typical experiment, 1M NaCl (1 mL), **2** (1 mL), 50 mM pH 5 phosphate buffer solution (2 mL), 1 mM methyl orange (1 mL) were mixed prior to the addition of a 10 mM oxone (HSO_5^-; 100 μL) solution. After two minutes, this was extracted with *n*-heptane. GC-MS analysis revealed monochlorodimethylaniline (*m*/*z* 154) and dichlorodimethylaniline (*m*/*z* 188), matching with calibration experiments using methyl orange and authentic hypochlorite. The estimated yields of OCl^- per mole of oxone were 85% at pH 5, 5.5% at pH 7.6, and 0.3% at pH 9.0.

[15] R. H. Holm, J. P. Donahue, *Polyhedron* **1993**, *12*, 571–589.

[16] J. Lee, J. A. Hunt, J. T. Groves, *J. Am. Chem. Soc.* **1998**, *120*, 7493–7501.

The High-Valent Compound of Cytochrome P450: The Nature of the Fe–S Bond and the Role of the Thiolate Ligand as an Internal Electron Donor**

François Ogliaro, Shimrit Cohen, Michael Filatov, Nathan Harris, and Sason Shaik*

Recently, Schlichting et al.[1] have used time-lapse X-ray crystallography to "photograph" the hydroxylation pathway of camphor by cytochrome $P450_{cam}$, which includes the elusive, high-valent iron-oxene species (**1** in Scheme 1a). In response to this exciting work, we present here an extensive density functional theoretical (DFT) investigation of iron

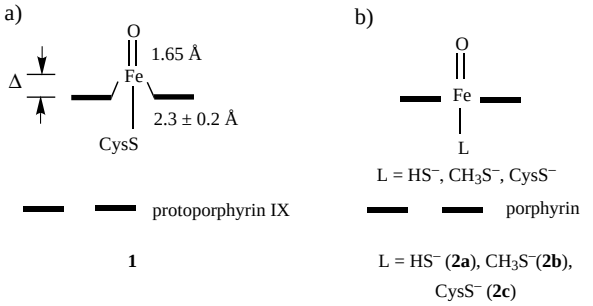

Scheme 1. Selected X-ray diffraction data for a) the high-valent P450 iron oxene species **1**. Δ indicates the protrusion of the iron center from the porphyrin plane. b) Model systems **2a–c**.

oxene (**2a–c**, Scheme 1b) with emphasis on geometry, electronic structure, and unusual features of the Fe–S bonding. Thus, while the X-ray diffracting species[1] qualitatively fits iron oxene, its precise geometric data are less certain. For example, the distance between the iron and the proximal ligand, $r_{Fe\text{-}S}$, appears quite short but the value 2.3 ± 0.2 Å has a significant uncertainty. Another uncertainty, discussed by the authors,[1] is the possible contamination by an additional species. Theory[2] itself has not as yet settled on a value for this distance, which appears to vary between 2.37–2.69 Å for different models systems and computational levels.[2] An associated issue is the theoretical characterization of the flexibility of the Fe–S linkage in **1** and the role of the thiolate ligand as an internal electron donor.[3] A still uncertain feature of P450 iron oxene is whether it involves a porphyrin cation radical, as in the analogous Compound I species of horseradish peroxidase[4a] and synthetic models,[4b] or, rather, does it possess a sulfur radical situation,[2a,e] or perhaps a resonance hybrid of these forms.[3, 5] A related question concerns the spin-state identity; high-spin as in some Compound I species,[4a,b] or low

[*] Prof. S. Shaik, Dr. F. Ogliaro, S. Cohen, Dr. M. Filatov, Dr. N. Harris
Department of Organic Chemistry and
The Lise Meitner-Minerva Center for
Computational Quantum Chemistry
Hebrew University, 91904 Jerusalem (Israel)
Fax: (+972) 2-6584680
E-mail: sason@yfaat.ch.huji.ac.il

[**] This research was sponsored in part by the Israeli Science Foundation (ISF) and the Binational German–Israeli Foundation (GIF). F.O. thanks the EU for a Marie Curie Fellowship.

spin as in chloro peroxidase.[4a] These issues, and the great interest in P450 iron oxene as a potent oxidizing agent,[5] call for a theoretical treatment focused on these points.

This paper presents a DFT study of the four lower-most states of Compound I for three different thiolate ligands (**2a**–**c** in Scheme 1b), as isolated molecules and in a polarizing medium. Calculations were done with the GAUSSIAN 98 package,[6] using the unrestricted hybrid-functional UB3LYP[7] with full geometry optimization. Four basis sets were used, labeled as B1 – B4.[8, 9] The least extensive, B1, uses an effective core potential and the double-zeta quality LACVP basis set.[8] The most extensive, B4, uses the all electron 6-311 + G* basis set.[6] Solvent calculations were carried out with the IEF-CPM model[10] implemented in GAUSSIAN,[6] which used a dielectric constant for water of $\varepsilon = 78$. The effect of a low dielectric constant was tested with the solvation with JAGUAR using $\varepsilon = 5.7$ (for C_6Cl_6).[11] The electric field and hydrogen bonding in the protein pocket are very important.[12] Our solvent calculation represents a simple way to approach the problem and we must emphasize that the calculations are intended only to reveal trends induced by medium polarization. As will be shown later, the trends for $\varepsilon = 5.7$ and $\varepsilon = 78$ are identical.

P450 iron oxene has four low-lying states, each of which is a tri-radicaloid, as depicted in Scheme 2. Two of the unpaired electrons occupy the π* orbitals of the ferryl group with a triplet overall spin. The third electron is coupled to the triplet

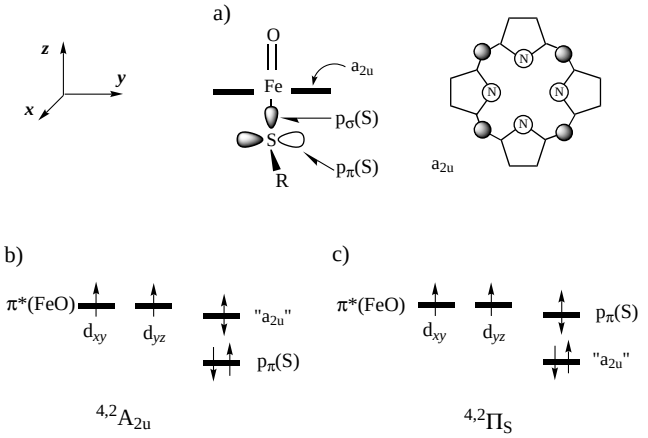

Scheme 2. Key orbitals and tri-radicaloid states of P450 iron oxene.

pair in either a ferromagnetic or antiferromagnetic manner, to give a quartet and doublet spin states.[2, 4] The $^{4,2}A_{2u}$ states (Scheme 2b) arise from a single occupation of the "a_{2u}" orbital, which is composed of the corresponding a_{2u} orbital of the free porphyrin mixed with the $p_\sigma(S)$ orbital (see Scheme 3a). The $^{4,2}\Pi_S$ states involve single occupation of the sulfur $p_\pi(S)$ orbital (Scheme 2c) mixed with the $d_{yz}(\pi^*(FeO))$ orbital. State characterization was achieved by a detailed inspection of the unrestricted Kohn – Sham orbitals and by transformation of these orbitals to the corresponding delocalized natural orbitals.[13] In C_1 symmetry, there is interstate mixing but the A_{2u} or Π_S parenthood is still recognizable by the natural orbital analysis.

The relative ordering of the four states derives from the relative π- versus σ-donor capability of the thiolate ligand with respect to the porphyrin (through its a_{2u} orbital) and, therefore, depends on the thiolate ligand, the porphyrin substituents, and the polarization due to electric field or hydrogen bonding in the protein pocket (which also possesses a water population[1, 12]). The three ligands of choice (**2a**–**c**) and the solvent calculations can reveal insight regarding these factors.

Table 1 shows the relative energies of the A_{2u} and Π_S state types for the different ligands at the optimized geometries.[8, 9] The energy spacing within the state types is much smaller (see Figure 1). It is seen that, while for $L = HS^-$ (**2a**) and $CysS^-$ (**2c**), the $A_{2u} - \Pi_S$ energy difference is appreciable; in the case of $L = CH_3S^-$ (**2b**), the four states are jammed into a space of about 1 kcal mol^{-1}. The CH_3S^- ligand, the best π-donor among the three ligands, over stabilizes the Π_S states relative to the A_{2u} states. Single-point values using the optimized $^4A_{2u}$ geometry for all the four states, are given in parentheses in Table 1 and show that the trend is independent of the precise geometric details of the different states. This trend persists even if the B3P86 functional is used instead of B3LYP. Thus, HS^- appears to be a more faithful mimic of the full $CysS^-$ ligand. This is apparent also from the Fe–S bond dissociation energies (see below). Thus, HS^- is the choice model ligand for $CysS^-$. As recently pointed out,[2c] an alternative model is one which uses $L = CH_3S^-$ but with the full protoporphyrin IX moiety. In this case, the porphyrin substituents level the relative donor abilities of the proximal ligand with respect to the porphyrin ring.

Table 1. $A_{2u} - \Pi_S$ energy gaps[a] for the model systems in different basis sets (B*i*). In parentheses are values obtained for a fixed geometry of the corresponding ground state.

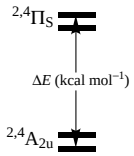

Basis set	L = HS^- (**2a**)	L = CH_3S^- (**2b**)	$CysS^-$ (**2c**)
B1	5.46 (6.17)	0.31 (1.68)	7.75 (7.86)
B2	4.86 (5.34)	0.20 (1.29)	– (6.81)
B3	5.33 (6.32)	0.66 (–)	– (–)

[a] In kcal mol^{-1}.

Figure 1 shows the two lowest states for the three ligands, in different basis sets and with a solvation effects included ($\varepsilon = 78$). In agreement with others,[2a,c,d] for **2b**, better basis sets and medium polarization favor the doublet state for all three ligands. Using the low dielectric constant ($\varepsilon = 5.7$) for **2a** gave precisely the same trend, preferring slightly the doublet state. This conclusion is in accord with EPR assignment[4] of the ground state in Compound I of chloro peroxidase. The *J* value[14] for **2a** in a solvent is -42 cm^{-1}, in accord with the EPR data[2e] (-37 cm^{-1}). Considering experimental uncertainties[2e] and the accuracy limits of the DFT method, this

  0044-8249/00/11221-4010 $ 17.50+.50/0

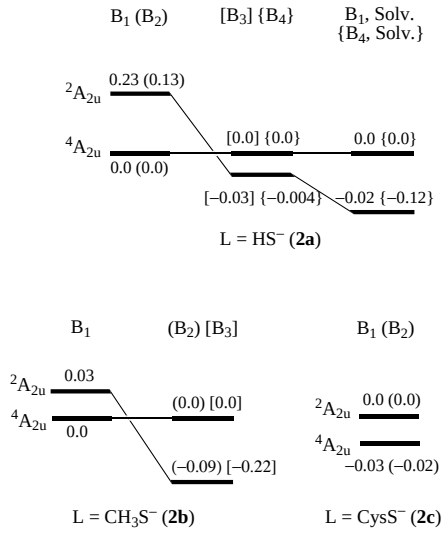

Figure 1. $^4A_{2u}-{}^2A_{2u}$ energy gaps for the model systems for different basis sets and with solvent polarization.

agreement must be taken with caution. A prudent conclusion, at this point, is that the two states are predicted by theory to be virtually degenerate. The factors involved in the choice of the ground state will be discussed later.

Figure 2 shows the geometries of A_{2u} states in different basis sets; in C_s symmetry for the first two ligands and in C_1 for the full cysteinato ligand. C_1 results for **2a** show that the C_1 and C_s geometries and energies are very close.[15] The geometric parameters of the FeO porphyrin moieties are almost invariant and agree with experimental estimates,[1] **1** in Scheme 1. Also in agreement is the protrusion of the Fe atom above the porphyrin plane, which itself undergoes a modest ruffling of a few degrees. The Fe–S bond (for the choice ligands HS^- and $CysS^-$) is about 0.3–0.4 Å longer than the experimental estimate. However, the discrepancy may not be all that large considering the experimental error bar (±0.2 Å).[1] The Fe–S distance varies with the donor capability of the ligand; it is the longest for **2b**[2d] and shortest for **2a**. The doublet state, as a rule, has a longer bond than the quartet state.[2c,d]

Figure 3a shows the state ordering as a function of the Fe–S distance for **2a**. At longer Fe–S distances (>2.7 Å), the ground state is $^2A_{2u}$, while at shorter distances the ground state is $^4A_{2u}$. Based on approaches for diradicaloids,[16, 4b] the

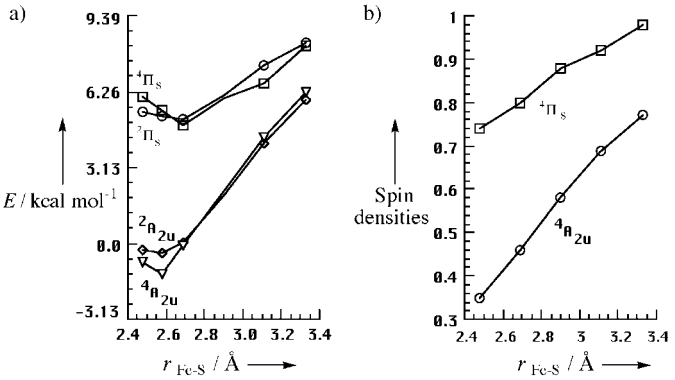

Figure 3. a) States energies (for **2a**; B1 level) as a function of the Fe–S distance. b) SH spin densities for $^4A_{2u}$ and $^4\Pi_S$ as a function of the Fe–S distance. The corresponding spin densities for the low-spin states are negative and have a mirror image behavior to the high-spin states.

major factor is the exchange integral, K_{ij}, of orbitals i and j which accommodate the unpaired electrons. High-spin states are favored by a large K_{ij}, as conferred when the two orbitals share common atoms. When the orbitals are disjointed, K_{ij} is small and the low-spin state will be favored by virtue of superior Coulomb correlation. By reference to Scheme 2, the two orbitals which will determine the ground state spin are the "a_{2u}" and d_{yz} orbitals (the in plane π^*_{FeO}). These orbitals are virtually disjointed and have a small exchange integral (Scheme 3a,b). However, since the two orbitals are of the same symmetry species, one expects some mixing, which is readily apparent by inspection of the natural "a_{2u}"-type orbital (Scheme 3c). The shorter the Fe–S distance, the stronger this admixture and the corresponding exchange integral $K_{\text{"}a_{2u}\text{"}-\pi^*}$ increasingly favors the high-spin $^4A_{2u}$ state. Thus, at short Fe–S distances, the $^4A_{2u}$ high-spin state is the ground state while at longer distances the low-spin $^2A_{2u}$ state is preferentially stabilized and becomes the ground state.[17a]

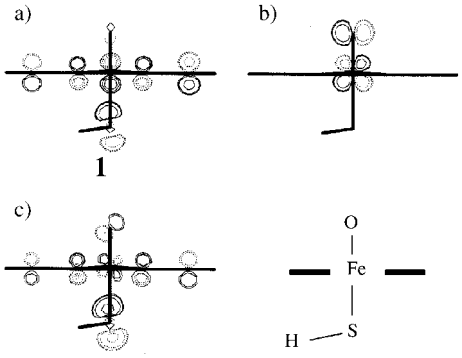

Scheme 3. Contour plots of a) the "a_{2u}" and b) π^*_{FeO} Kohn–Sham orbitals, and c) the natural "a_{2u}" orbital.

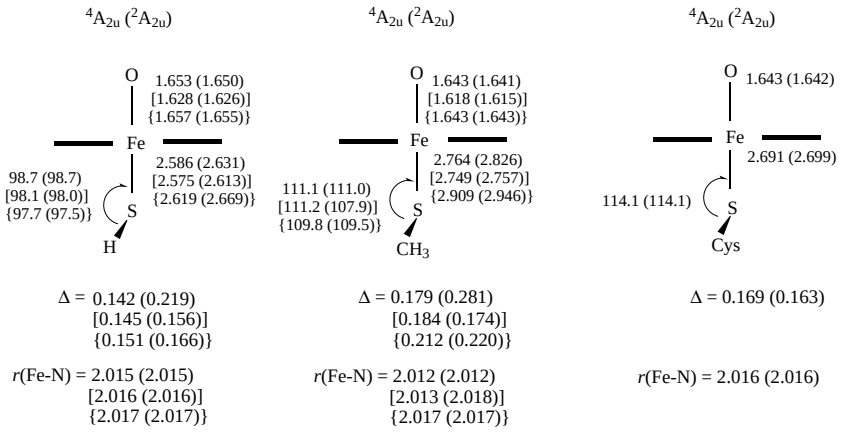

Figure 2. Optimized geometries for the $^4A_{2u}$ and $^2A_{2u}$ states of the model systems (C_s[15] for HS^- and CH_3S^-, and C_1 for $CysS^-$). Unbracketed values correspond to B1; those in square brackets to B2, and those in curly brackets to B3. The Δ values [Å] correspond to the protrusion of the Fe atom above the porphyrin plane; r(Fe–N) is the average bond length.

Since the spin identity of the ground state depends on the Fe–S bond distance, one wonders how variable is the bond length. As seen in Figure 3a, a displacement of the Fe–S bond over 1 Å, costs about 6 kcal mol^{-1} (at most, since we did not allow for geometric relaxation during stretching). Especially soft is the direction of bond shortening from 2.8 →2.4 Å which requires about 1 kcal mol^{-1}. Clearly, thiolate enzymes, with different constraints on Fe–S distance and differing proximal pocket polarities which attenuate the donor ability of the thiolate[12] will possess slightly different Fe–S bond distances and have either $^4A_{2u}$ or $^2A_{2u}$ as ground states. A spin state equilibrium[3c] or mixed-spin state situations are likely.

The fluxionality of the Fe–S bond is rooted in the thiolate spin-density variation in Figure 3b, which shows that the A_{2u} spin density starts as approximately 0.5 e at short distances and increases with Fe–S elongation. Thus, the Fe–S bond elongation is attended by internal charge transfer from the thiolate toward the porphyrin "hole". In fact, iron oxene dissociates into the neutral (porphyrin)FeO and the thiolyl radical, with effectively a very small bond dissociation energy D of 6.3 (**2c**), 6.9 (**2a**), and 3.0 kcal mol^{-1} (**2b**). As shown in Scheme 4, the bond dissociation involves a crossing of

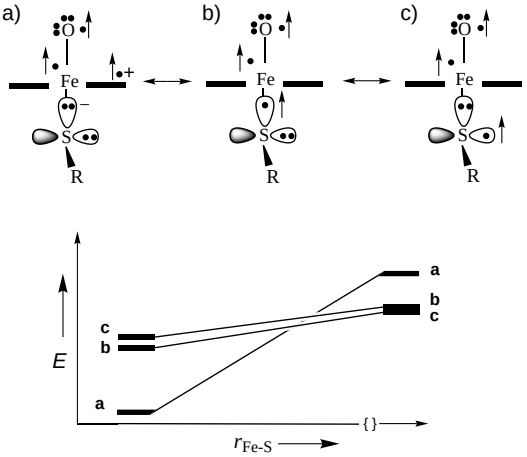

Scheme 4. Resonance contributors to the electronic structure of P450 iron oxene and their relative energies as a function of the Fe–S distance.

resonance structures;[3a,d, 5b,c] one (a) involves a thiolate anionic state and the other (b) involves a σ-thiolyl radical situation. At shorter distances (< 2.6 Å) both (a) and (b) mix and contribute to the electronic structure. As the Fe–S bond becomes longer, the thiolyl radical structure (b) is stabilized and eventually crosses below (a). Another form, (c), nascent from the Π_S states, will also cross as it is virtually degenerate with (b) at the dissociation limit. The three forms mix, avoid the crossing, and thereby induce a flat potential and an effectively weak bond energy. The role of such resonance forms, termed also "redox tautomerism",[3d] has been postulated based on experimental findings[3a,d, 5b,c] and is supported here by theoretical calculations. The imprint of this mechanism should be tractable, as demonstrated by vibrational spectroscopy of the high-spin ferric form of $P450_{cam}$.[3b]

In summary, the Fe–S bond of Compound I has a small bond dissociation energy (6 – 7 kcal mol^{-1}) and is flexible, due to internal charge transfer from the thiolate to the porphyrin ring. Our solvent calculations show that, irrespective of dielectric constant, the polarization of the medium reduces the thiolate spin density. Should the same effect be exerted within the protein pocket,[3c] then, based on the relation in Figure 3b, some shortening of the Fe–S bond would be expected. Such an effect, imparted by hydrogen bonding, has been demonstrated recently in model compounds.[12f] It follows also that isoforms of P450 and related thiolate enzymes (like CPO, NOS, and so forth), which differ in their pocket polarities[12b,c] and acidities may possess different Fe–S characters and spin situations. This prediction merits appropriate computational tests.

As pointed out, the C_1 symmetry will cause some $\Pi_S - A_{2u}$ state mixing, due to rehybridization of the $p_\pi(S)$ and $p_\sigma(S)$ orbitals. This mixing will increase as the Fe–S bond stretches and tilts off axis in the C_s plane (Scheme 4).[17b] Significant spin-orbit coupling conferred by the sulfur atom will further enhance the rate of spin-state transitions through $^{2,4}\Pi_S - {}^{4,2}A_{2u}$ mixing.[5b, 17c] This latter feature, as well as the bond flexibility, are likely to have an impact on the oxidative reactions of Compound I.[2d, 18]

Received: April 13, 2000
Revised: August 2, 2000 [Z 14990]

[1] I. Schlichting, J. Berendzen, K. Chu, A. M. Stock, S. A. Maves, D. A. Benson, R. M. Sweet, D. Ringe, G. A. Petsko, S. G. Sligar, *Science* **2000**, *287*, 1615.
[2] a) M. T. Green, *J. Am. Chem. Soc.* **1999**, *121*, 7939; b) D. L. Harris, G. H. Loew, *J. Am. Chem. Soc.* **1998**, *120*, 8941; c) D. L. Harris, G. H. Loew, *Chem. Rev.* **2000**, *100*, 407; d) M. Filatov, N. Harris, S. Shaik, *J. Chem. Soc. Perkin Trans. 2* **1999**, 399; e) J. Antony, M. Grodzicki, A. X. Trautwein, *J. Phys. Chem. A* **1997**, *101*, 2692.
[3] a) J. H. Dawson, M. Sono, *Chem. Rev.* **1987**, 1255; b) P. M. Champion, *J. Am. Chem. Soc.* **1989**, *111*, 3433; O. Bangcharoenpaurpong, P. M. Champion, S. A. Martinis, S. G. Sligar, *J. Chem. Phys.* **1987**, *87*, 4273; c) M. Unno, J. F. Christian, D. E. Benson, N. C. Gerber, S. G. Sligar, P. M. Champion, *J. Am. Chem. Soc.* **1997**, *119*, 6614; d) J. Bernadou, A.-S. Fabiano, A. Robert, B. Meunier, *J. Am. Chem. Soc*. **1994**, *116*, 9375.
[4] a) C. E. Schulz, R. Rutter, J. T. Sage, P. G. Debrunner, L. P. Hager, *Biochemistry* **1984**, *23*, 4734; b) E. Bill, X.-Q. Ding, A. X. Trautwein, H. Winkler, D. Mandon, R. Weiss, A. Gold, K. Jayaraj, W. E. Hatfiled, M. L. Kirk, *Eur. J. Biochem.* **1990**, *188*, 665.
[5] a) J. T. Groves, Y.-Z. Hang in *Cytochrome P450: Structure, Mechanisms and Biochemistry*, 2nd ed. (Ed.: P. R. Ortiz de Montellano), Plenum, New York, **1995**, chap. 1; b) W.-D. Woggon, *Top. Curr. Chem.* **1996**, *184*, 40; c) M. Sono, M. P. Roach, E. D. Coulter, J. H. Dawson, *Chem Rev.* **1996**, *96*, 2841.
[6] *GAUSSIAN98*, Gaussian, Inc., Pittsburgh PA, **1998**.
[7] P. J. Stevens, F. J. Devlin, C. F. Chablowski, M. J. Frisch, *J. Phys. Chem*. **1994**, *98*, 11623.
[8] LACVP: J. P. Hay, W. R. Wadt, *J. Chem. Phys.* **1985**, *82*, 299.
[9] a) B2 is generated from LACVP by adding polarization functions on the heavy atoms, LACVP*; b) B3 is 6-311 + G.
[10] E. Canes, B. Mennucci, J. Tomasi, *J. Chem. Phys.* **1997**, *107*, 3032.
[11] JAGUAR 3.5, Schrödinger, Inc, Portland, Oregon. This is an improved solvent model, analogous to PCM but with a different implementation than in GAUSSIAN. See its performance in: B. Marten, K. Kim, C. Cortis, R. A. Friesner, R. B. Murphy, M. N. Ringnalda, D. Sitkoff, B. Honig, *J. Phys. Chem.* **1996**, *100*, 11775. See also its application to bacteriochlorophyll and bacteriopheophytin in: L. Y. Zhang, R. A. Friesner, *J. Phys. Chem.* **1995**, *99*, 16479.
[12] a) The proximal pocket involves hydrogen bonds to the cysteinato sulfur and the postive ends of the local dipoles are oriented toward it

  0044-8249/00/11221-4012 $ 17.50+.50/0

(T. L. Poulos, J. C. Vickery, H. Li in *Cytochrome P450: Structure, Mechanisms and Biochemistry*, 2nd ed. (Ed.: P. R. Ortiz de Montellano), Plenum, New York, **1995**, chap. 6). This will further make the donor ability of the cysteinato ligand similar to HS^-; b) both CPO and iNOS are known to possess more extensive hydrogen bonding to the cysteinato ligand and thereby weaken its interaction with the iron (D. L. Wang, D. J. Stuer, D. L. Rousseau, *Biochemistry* **1997**, *36*, 4595). In iNOS there is aromatic stacking which may stabilize the A_{2u} states with a prominent porphyrin hole (B. R. Crane, A. S. Arvai, R. Gacuchhui, C. Wu, D. Ghosh, E. D. Getzhoff, D. J. Stuehr, J. A. Tainer, *Science* **1997**, *278*, 425); c) for related discussions, see: H. Aissaoui, R. Bachmann, A. Schweiger, W.-D. Woggon, *Angew. Chem.* **1998**, *110*, 3191; *Angew. Chem. Int. Ed.* **1998**, *37*, 2998; D.Harris, G. H. Loew, *J. Am. Chem. Soc.* **1993**, *115*, 8775; d) to mimic the electric potential at the thiolate site, one needs electropositive moieties in model systems. See: H.-A. Wagenknecht, C. Claude, W.-D. Woggon, *Helv. Chim. Acta* **1998** *81*, 1506; e) for recent mutation that probe the distal and proximal pockets, see: M. P. Roach, A. E. Pond, M. R. Thomas, S. G. Boxer, J. H. Dawson, *J. Am. Chem. Soc.* **1999**, *121*, 12088; f) NH–S hydrogen bonding shortens the Fe–S bond in a synthetic model. See: N. Suzuki, T. Higuchi, Y. Urano, K. Kikuchi, H. Uekusa, Y. Ohashi, T. Uchida, T. Kitagawa, T. Nagano, *J. Am. Chem. Soc.* **1999**, *121*, 11571.

[13] E. D. Glendening, J. Badenhoop, A. E. Reed, J. E. Carpenter, F. Weinhold, Theoretical Chemistry Institute, University of Wisconsin, Madison, USA (NBO v.4.0). The natural orbital analysis identifies the three singly occupied orbitals (Scheme 2) and facilitates the states identification relative to the more tedious analysis of the UKS orbitals.

[14] J is evaluated using the formulae ($\boldsymbol{H}_{spin} = -J\boldsymbol{S}_1\boldsymbol{S}_2$), given in L. Noodleman, D. A. Case, *Adv. Inorg. Chem.* **1992** *38*, 423.

[15] For example, with basis set B1, the C_1 geometric parameters of the $^4A_{2u}$ ($^2A_{2u}$) states for **2a** are $r_{FeO} = 1.651$ (1.648), $r_{FeS} = 2.581$ (2.600), and $\Delta = 0.143$ (0.154) Å. The $^4A_{2u}$ ($^2A_{2u}$) energy difference is $+0.09$ kcal mol^{-1}. The main deviation from C_s symmetry is a tilt of the Fe–S axis off the C_s plane of symmetry and the energy stabilization of C_1 relative to C_s is small <1 kcal mol^{-1}.

[16] W. T. Borden in *Encyclopedia of Computational Chemistry*, *Vol. 1* (Eds.: P. von R. Schleyer, N. L. Allinger, T. Clark, J. Gasteiger, P. A. Kollman, H. F. Schaefer III, P. R. Schreiner), Wiley, Chichester, **1998**, p. 708.

[17] a) In the low-spin situation, the two natural orbitals form bonding and antibonding combinations; b) In C_1 some $A_{2u} - A_{1u}$ admixture is also expected. The A_{2u} parenthood is still apparent though in the calculation and the corresponding A_{1u} states are slightly higher in energy than the Π_S states; c) The perpendicular relation of the $p_\sigma(S)$ and $p_\pi(S)$ orbitals provides significant one center contribution to spin orbit coupling (SOC). A simple perturbation treatment of SOC ($\zeta_S = 388$ cm^{-1} and an energy gap taken from Figure 1) leads to a mixing coefficient of 0.14–0.18 from the quartet into the doublet state.

[18] N. Harris, S. Cohen, M. Filatov, F. Ogliaro, S. Shaik, *Angew. Chem.* **200**, *112*, 2070; *Angew. Chem. Int. Ed.* **2000**, *39*, 2003.

Formation of Novel Ordered Mesoporous Silicas with Square Channels and Their Direct Observation by Transmission Electron Microscopy**

Tatsuo Kimura, Takayuki Kamata, Minekazu Fuziwara, Yuri Takano, Mizue Kaneda, Yasuhiro Sakamoto, Osamu Terasaki, Yoshiyuki Sugahara, and Kazuyuki Kuroda*

Since the discovery of an ordered mesoporous silica,[1] the preparation of various mesoporous silicas by using surfactant assemblies has been developed.[2–4] These mesoporous silicas have proved to be highly applicable as catalysts, catalyst supports, and adsorbents for relatively large molecules,[5] which has stimulated a number of studies including both morphological control[6, 7] and compositional variations.[3, 8, 9] However, all the structures reported so far have been governed by the geometrical packing of surfactants[4, 10] because the formation of the mesostructured precursors relies on the cooperative organization of inorganic species and surfactants.[11] Herein, we report on the formation of novel mesoporous silicas (denoted as KSW-2) with rectangular arrangements of square or lozenge one-dimensional (1D) channels by mild acid treatment of a layered alkyltrimethylammonium (C_nTMA)–kanemite complex. Mesostructured precursors of KSW-2 formed through the bending of individual silicate sheets of kanemite. The square or lozenge shape of the relatively ordered pores has not previously been found among the reported mesoporous and mesostructured inorganic oxides.

Kanemite ($NaHSi_2O_5 \cdot 3H_2O$), a mineral, is made up of layered polysilicates composed of SiO_4 tetrahedral units,[12] and the crystal structure was recently determined by Gies et al.[13] Kanemite is a layered silicate composed of single sheets such as δ-$Na_2Si_2O_5$ and $KHSi_2O_5$; the sheets are constructed by connecting 6-rings of SiO_4 tetrahedra wrinkled

[*] Prof. Dr. K. Kuroda,[+] Dr. T. Kimura, T. Kamata, Y. Takano, Prof. Dr. Y. Sugahara
Department of Applied Chemistry, Waseda University
Ohkubo 3-4-1, Shinjuku-ku, Tokyo 169-8555 (Japan)
Fax: (+81) 3-5286-3199
E-mail: kuroda@mn.waseda.ac.jp

[+] Kagami Memorial Laboratory for Materials Science and Technology
Waseda University, Nishiwaseda 2-8-26, Shinjuku-ku, Tokyo 169-0051 (Japan)

M. Fuziwara
Materials Characterization Central Laboratory, Waseda University
Ohkubo 3-4-1, Shinjuku-ku, Tokyo 169-8555 (Japan)

M. Kaneda, Dr. Y. Sakamoto, Prof. Dr. O. Terasaki
Department of Physics, Graduate School of Science
Tohoku University, Sendai, 980-8578 (Japan)

Prof. Dr. O. Terasaki
CREST, JST and Center for Interdisciplinary Research
Tohoku University, Sendai, 980-8578 (Japan)

[**] This work was supported by CREST, Japan Science and Technology Corporation, and Grant-in-Aid for the Scientific Research from the Ministry of Education, Science, Sports, and Culture of the Japanese Government.

Supporting information for this article is available on the WWW under http://www.wiley-vch.de/home/angewandte/ or from the author.